Groundwater for Sustainable Development, Vol. 26, 101270, 2024, doi:10.1016/j.gsd.2024.101270.

Satellite gravimetry observations on the state of groundwater level variability in the Arabian Peninsula Region and the associated socio-economic sustainability challenges

Muhammad Usman[a] & Kosuke Heki[b,c]

[a]*Dept. Environmental Sciences and Sustainability, College of Natural and Health Sci., Zayed Univ., Abu Dhabi, UAE*

[b]*Dept. Earth Planet. Sci., Hokkaido Univ., N10 W8, Kita-ku, Sapporo, Hokkaido 060-0810, Japan*

[c]*Chinese Acad. Sci., Shanghai Astronomical Obs., Shanghai China*

Abstract

Groundwater is an important resource for the Arabian Peninsula Region. The population increase, rise in agricultural activities, and Gulf Cooperation Council (GCC) countries (Bahrain, Kuwait, Oman, Qatar, Saudi Arabia, and the United Arab Emirates) inclination towards economic diversification and tourism promotion have heightened the freshwater demand. As a result of climate change and varying weather patterns, the situation has become more complicated. Due to arid conditions, recharge is mostly less than withdrawal which consequently results in underground water level decline over time. In the research, we have used Gravity Recovery and Climate Experiment (GRACE/GRACE-FO) MASCON solutions, Global Land Data Assimilation System (GLDAS) soil moisture, and the Integrated Multi-satellite Retrievals for Global Precipitation Mission (IMERG) rainfall data to observe the Equivalent Water Thickness (EWT), and rainfall patterns in this region for the past two decades (2002-2023). The results indicate that in Saudi Arabia the water level is declining nearly at a linear rate and the linear regression model fits well with the data (R^2 value, the coefficient of determination, for different cities of Saudi Arabia is ≥ 0.94). In the Al Jouf Area, the water decline is the highest at -1.69cm/year which is 43% greater than the previous calculations. The lowest decline rate is in Sanaa (Yemen) which is -0.13cm/year. Furthermore, all the other studied locations show a groundwater declining trend. In Saudi Arabia's Makkah, Madina, Riyadh, and Damam the reduction rate is -0.36, -0.48, -0.72, and -0.48 (cm/year) respectively. Kuwait, UAE's

Dubai, and Al Ain show a similar groundwater reduction rate of -0.19cm/year. In Oman's Masqat, the groundwater decline rate is -0.22cm/year. Also, in the recent data, one can see the higher seasonal amplitudes that are indicative of greater fluctuations in EWT data in recent times. If water mining continues at the same pace, this important resource can become a rare commodity. Limited water supply can likely become a limiting factor for further social, agricultural, and industrial development. That's why major reviews and shifts are necessary in the current policies related to water resource management and conservation.

1. Introduction

Water carries huge significance for humans and the ecosystem, and the sustainability of water is a challenging issue globally (United Nations, 2013; Bernauer and Böhmelt, 2020). Groundwater is the third-biggest water resource and largest source of fresh water on Earth (Kong et al., 2022) and more than two billion people around the world solely depend on this significant water resource for drinking purposes (Doll, 2009; Boretti and Rosa, 2019; Gronwall and Danert, 2020). However, in the present times, the intensive use of groundwater, caused by anthropogenic activities, has affected this important natural resource (Wada et al., 2010, Scanlon et al., 2023).

The accelerating per capita water demand is related to the high population growth and increase in living standards (Water UN 2012; Boretti and Rosa, 2019). The population growth triggers a simultaneous increase in water demand in various sectors including domestic, agriculture, and industry (Hatamkhani et al. 2022). The population growth in the Arab Peninsula's population is considered one of the highest in the world (Odhiambo, 2016). During the last four decades, the discovery of oil and gas reserves has resulted in these countries' oil revenues, and it laid a foundation for a strong economic base and rapid improvement in the standard of living in the Arabian Gulf countries (Mirkin, 2010). The population of the GCC countries grew at an average annual rate of 14% and the GDP increased at an average annual rate of 5.2% during the same period of 1998 to 2008 (EIU, 2010). From 1970 to 1990 the population in the countries of the region increased from 17.8 to 33.5 million which is almost twofold in just two decades (Water UN, 2012).

The significant increase in economic activity in the GCC countries has resulted in an increased demand for the workforce, and there is a large inflow of the immigrant population. In the Arabian Peninsula Region, the population is now over 77.9 million (World Population Review, 2024). Data shows that the expatriate population in GCC countries can range from 25% in Oman to 90% in the

UAE (World Bank, 2005). It is projected that the population of GCC countries will rise to 120 million by 2050 (UNESCO, 2003). The overall per capita freshwater availability fell from about 680 m^3 in 1970 to about 180 m^3 in 2000, and now it is below 100 m^3 in various GCC countries. To ensure sustainable development, it is vital to sustain resources in such a way that they can meet the ever-increasing demand for energy and freshwater (Bachellerie, 2012). With the current rate of population increase and water management procedures and use practices, the annual water demand may exceed 50 BCM by 2030 (Al-Zubari, 1997). It is expected that in the future desalination and wastewater re-use capacity will stay limited (Chowdhury and Champagne, 2006), and the freshwater demand will have to be met mainly by further mining of groundwater reserves which are now declining at a rapid pace (Odhiambo, 2016). Under these circumstances, it becomes essential to maintain a precise look at this important resource. It will help us make effective policies to achieve sustainability and sustainable development.

Excessive withdrawals can cause groundwater levels to decline and this phenomenon has been observed in various parts of the world (Rodel et al. 2018). In the arid regions, agriculture is the main sector where groundwater is utilized. It accounts for 70% of water extraction and 90% of water consumption (Siebert et al., 2010; Gerten et al., 2020). Due to the extensive withdrawal and limited recharge, water shortage has become a serious problem for different countries in the Arab Region (Mohamed et al. 2022). So, to address the issue of water sustainability, it has become important to maintain a balance between population growth, economic development, land management, and climate change (Trondalen, 2009). Furthermore, Middle Eastern countries are being affected by desertification and it has already become a serious issue in Iraq, Syria, Jordan, and Iran (Mohamed et al. 2022).

The groundwater level decline is a regional issue and the extraction of groundwater takes place over a large spatial coverage. On the other hand, the conventional in-situ methods can provide only limited insight into this broad issue (Mohamed et al. 2022). Rodell and Famiglietti (2001) anticipated that the Gravity Recovery and Climate Experiment (GRACE) would be powerful enough to examine Terrestrial Water Storage (TWS) over a larger basin area of 200,000 km^2. Now, many researchers utilize the GRACE data in various parts of the world and produce important findings. The GRACE data has been used to study the mass losses in ice sheets and glaciers (e.g., Velocogna and Wahr, 2005; Wouter et al. 2008; Velincogna, 2009; Velinconga et al. 2020; Hata et al: 2022; Wang et al. 2023), co- and postseismic gravity changes (e.g., Tanaka and Heki, 2014; Tanaka et al. 2015), drought and TWS change (e.g., Xavier et al. 2010; Long et al. 2013; Long et al. 2014; Landrer et al. 2020; Moghim 2020;

Arora et al. 2022; Alshehri and Mohamed, 2023), as well as land subsidence due to groundwater over-pumping (Othman, 2019; Othman and Abotalib, 2019).

The vertically integrated terrestrial water storage (ΔTWS) changes from a regional to a global scale are monitored by the GRACE satellites. Some previous studies provide insight into the ΔTWS in and around the Arabian peninsula (Fallatah et al. 2017; Fallatah et al. 2019; Muhammad et al. 2022; AslShehri and Mohamed, 2023). However, no such studies have investigated the detailed spatiotemporal evolution of TWS for the highest gravity decline area that covers the Al Jouf and Riyadh regions, and the water reserves here carry huge significance for Saudi Arabia. Having a precise knowledge of water reserves in this arid environment is important for planning future agricultural activities, irrigation, and domestic use. In this research, we not only updated the previous studies' results but also conducted a detailed space-time analysis along the profile of maximum EWT variability for a profile that covers a 1776-kilometer region. Furthermore, we also conducted a time-series analysis of different major urban settlements of the Arabian Peninsula Region. To fully understand the severity of the issue, it is essential to have a precise look and this can be achieved by running models on the seasonal components and secular trends separately. To achieve this, we segregate the intra-annual (cyclic) and long-period components so that any bias coming from the cyclic signal during the long-period component analysis is removed (Jensen et al. 2015). Moreover, once the intra-annual cyclic and long-period components are separated, it also enables us to study the contribution of each component with a clear insight.

The decline in the water reserves is a result of increased withdrawal for irrigation which is related to enhanced anthropogenic activities. To establish a horizontal connection between the different pillars of sustainability we also integrate our results and findings with the socio-economic dimensions as well.

2. Data and Methodology

For this research, we have not only focused on the major decline area of Equivalent Water Thickness (EWT) (Saq aquifer) but also studied the EWT variability for the nine major locations in the Arabian Penisula Region (Figure 1).

2.1. Datasets Utilised

2.1.1. Gravity Recovery and Climate Experiment (GRACE/GRACE-FO) Data

Launched in March 2002, GRACE is a cooperative NASA/DLR mission that maps the static and temporal global gravity fields of Earth (Tapley et al., 2004). Total vertically integrated terrestrial water storage (Wahr et al., 1998) spatiotemporal fluctuations are directly related to variations in Earth's gravity field variability. In this research, we utilized monthly mass concentration (mascons; release 06, version 2; 0.25° × 0.25° grid) GRACE-derived TWS solutions produced by the University of Texas Center for Space Research (UT-CSR) (Save et al, 2016) (CSR RL06 v02) (https://www2.csr.utexas.edu/grace/RL06_mascons.html). In MASCON data, the ellipsoidal correction for mass anomaly grid representation has been applied (Ditmar, 2018). To reduce leakages of the signals, this correction was applied separately for land and ocean. Various studies demonstrated the mascon solutions provide a higher spatial resolution, signal-to-noise ratio, and a reduced error compared to other solutions (e.g., spherical harmonics) and do not require de-striping, spatial smoothing, or any empirical scaling techniques (Luthcke et al., 2013; Watkins et al., 2015; Save et al., 2016; Wiese et al., 2016; Scanlon et al., 2016).

2.1.2. Global Land Data Assimilation System (GLDAS) and The Integrated Multi-satellite Retrievals for GPM (IMERG) Datasets

The GLDAS datasets (https://disc.gsfc.nasa.gov/datasets?keywords=GLDAS) are generated using various state-of-the-art remote sensing and ground-based datasets. It has a spatial resolution of 1 to 25 degrees. The GLDAS initiative (Rodell et al., 2004), utilizes four land-surface models e.g., the Catchment land surface model (CLSM), VIC, Noah, and Mosaic (Koster and Suarez, 1996; Liang et al., 1996; Koren et. al. 1999; Dai et al. 2003; Rodell et al., 2004) are run offline from atmospheric models over the period from 1948 to present (near real-time). Each model simulates soil moisture (SM) at different soil layers. In this research, we used monthly GLDAS data (GLDAS_NOAH025_M) with a spatial resolution of 0.25^0x0.25^0.

The rainfall data has a spatial resolution of 0.1^0x0.1^0 and is provided in various temporal resolutions, we have utilized mm/month data (GPM_3IMERGM, V07). Further information for the data product can be accessed from the link https://giovanni.gsfc.nasa.gov/giovanni/.

2.2. Methodology

For the GRACE/GRACE-FO data, first, we have calculated the mean gravity changes using the entire data from 2002 to 2023 (Figure 2). The GRACE/GRACE-FO measures equivalent water thickness (EWT), which is also referred to as terrestrial water storage (TWS). The groundwater storage change can be calculated by subtracting the soil moisture signal from EWT. In response to the seasonal rainfall the soil moisture has a strong seasonal signal and there is no significant long-term change (~21 years in this case) in trend (Figure S1). GLDAS data is complete while GRACE/GRACE-FO data has temporal gaps. In this arid region, the seasonal input has a minimal effect on the water storage and the annual withdrawal rate is expected to be linear. Furthermore, simulated data will also have some uncertainties so, treatment of temporal gaps in this region will have a limited effect on the results. Moreover, it is observed that GRACE and GRACE-FO data fit nicely and conclusions can be drawn without filling the temporal gaps (Hata et al. 2022). To estimate groundwater storage, we subtracted EWT GRACE/GRACE-FO from GLDAS soil moisture data and then decomposed the time series and modeled both seasonal and trend components. Furthermore, in this kind of arid region, every component of water carries significance so if even some soil moisture trend signals stay in the EWT, the analysis of the trend will provide an insight into the cumulative loss or gain of this important resource over a long-term scale.

The GRACE/GRACE-FO MASCON solutions data values are stored in netCDF (.nc) format and provided at the intersection of the point of 0.25^0x0.25^0 degree nodes. Our algorithm extracts values along the profile of Figure 1 in such a way that it selects the closest nodal point at every 10-kilometer (~0.1^0) distance thus minimizing the chance of missing any data point along the transect (Figure 3). We are interested in the long-period (inter-annual) and short-period (intra-annual) components, and these signals dominate the time series data in the Arabian Peninsula. Furthermore, the short-period (cyclic) and long-period signals were separated using the Hodrick–Prescott filter (Hodrick and Prescot, 1997). We have separated the two to ensure stationarity in each component and to eliminate the chances of bias associated with cyclic (when modeling the long-period component) and long-period (when modeling the cyclic component) components.

$$y_t = \tau_t + c_t + \varepsilon_t \text{ ---(1)}$$

$$\min_{\tau}\left(\sum_{t=1}^{T}(y_t - \tau_t)^2 + \lambda \sum_{t=2}^{T-1}[(\tau_{t+1} - \tau_t) - (\tau_t - \tau_{t-1})]^2\right) \text{ --- (2)}$$

In equation (1), the y_t is the original time series, τ_t is the trend component, c_t is the cyclic component and ε_t is the error. In equation (2) the first term is the cyclic component the second term is the trend component and λ is the smoothing parameter. For monthly data, the value of λ was set at 129,600 (Ravn and Ohlig, 2002). After decomposing the time series into the seasonal and trend components, we modeled the seasonal component (least square fit equation (3)) and also calculated the coefficients of annual and semiannual sines and cosines. The coefficients can be applied in the following equation (4) to regenerate the seasonal models.

$$G_t = a_1 + a_2\, t + \alpha \sin(2\pi t + \theta_1) + \beta \sin(4\pi t + \theta_2) \text{ ---(3)}$$

$$c_t = A \cos 2\pi t + B\sin 2\pi t + C\cos 4\pi t + D\sin 4\pi t\text{--- (4)}$$

In the equation (3), $a_1, a_2, \alpha, \beta, \theta_1$ *and* θ_2 are constants, the third and forth terms are annual and semi-annual seasonal changes, respectively.

In equation (4), c_t is the seasonal component and t is the time. The calculated coefficients A, B, C, and D are given in Figures 6 and 7.

As the trend in most of the datasets for different cities of the Arabian Peninsula is linear (Figure 6 and Figure 8) we have used the linear regression model to calculate the monthly Equivalent Water Thickness (EWT) variability.

$$y = mx + c\text{---(5)}$$

In the above equation the slope m gives the rate of change per month and when multiplied by the number of observations provides us the total decline during the entire study duration. The R^2 provides a value of how the best model fits with the data.

Furthermore, we created an animation (Figure S2) for the study area using all the available MASCON data.

3. Results and Discussion

3.1. The current state of water reserves at different locations in the Arabian Peninsula Region

Figure 2 exhibits the mean seasonal variability in the Arabian Peninsula Region. We have extracted the intra-annual (short-period) component using the HP filter and have calculated the mean for each month using all the available data. Figure 3 indicates the spatio-temporal EWT variability along the entire length of signal propagation. Figures 4 and 5 exhibit the long-period and short-period components, which were extracted using the HP filter. Figure 6 indicates the original time series, short-period (largely seasonal), and long-period components for the Al Jouf Region of Saudi Arabia. Figure 7 indicates the intra-annual component and its model while Figure 8 indicates the long-period component and the associated linear regression model. Figure 9 shows the overlay of EWT and rainfall data at different cities of the Arabian Peninsula (please see Figure 1 for locations).

Figure 1 shows that the strong EWT decline signal within the Arabian Peninsula covers the southeastern part of Jordan and Al Jouf and Riyadh province of Saudi Arabia. Figure 2 indicates that during the winter months (within the Arabian Peninsula Region) especially starting from January the

EWT signal starts to become stronger gradually till June, and from July the EWT signal starts to become weaker. One can also find a similar kind of seasonal behavior in Iran. The reason can be the fact that winter precipitation dominates these regions (Attada et al. 2022; Daneshvar et al. 2019) which results in the EWT signal becoming positive in the winter months.

Figure S2 provides the time-lapse (spatiotemporal) insight into the EWT change in the study region. One can observe that, as we cross the year 2008, the negative EWT signal for the Arabian Region starts to become visible in the Al Jouf area, and then in the start (for a couple of years), it diminishes in the winter months (i.e. after around December) and reappears in the summertime (i.e. after around June). Similar to our studies, Arora et al (2022) observed that in the part of Indus Basin, there were complete negative trends after 2008, which they referred to as the deficit of both TWS and Ground Water Storage (GWS). Over time, the negative values become stronger and the seasonality component starts to become less visible due to higher magnitude negative EWT coming from the long-period component. However, one can see that the negative values get diluted as we enter the wintertime. Furthermore, the negative values in the Al Jouf and Riyadh Region have higher magnitudes in the recent data so the decline signals coming from other locations of the Arabian Peninsula region are also not much noticeable. However, for the nine locations of the study area, their short and long-period signals become quite visible in the time series data as indicated in Figures 7 and 8.

Figure 3 indicates the spatiotemporal variability of the EWT signal extracted along the Al Jouf-Riyadh Transect (Figure 1). In this Figure, one can see how the signal propagates in space with the passage of time. Taking the 900-kilometer point as the center, one can observe that EWT decline signals move faster in the region between 0 to 900 km (towards Al Jouf and Jordan, Figure 3, panel a) than in the region between 900 to 1800 km (towards Riyadh, Figure 3, panel b). The major reason can be the extensive water withdrawal for irrigation purposes and extensive water extraction has resulted in a significant drop in the water table for up to 150 meters in this region towards Jordan (including Al Jouf area) (Othman and Abotalib, 2019). Figure 3 contains both cyclic (short-period) and long-period signals and one can observe that due to a high decrease in long-period, the short-period signal gets masked. So, we have applied, the HP filter and have separated the both long-period signal (Figure 4) and the cyclic signal (Figure 5). The observation of the long-period signals indicates the same speed of signal propagation as it was in Figure 3. However, one can see that after extracting the cyclic component, long-period values become more diluted in the areas between 900 to 1800 kms as compared to Figure 2 in the time between 2018 to onwards. It suggests that the cyclic component has a negative trend in recent times and it is also visible in the short-period component (Figure 5) for the same length and time. Also, in Figure 5 one can see a clear high variability in the seasonal signal for the entire length of 1800 kilometers in the GRACE-FO data (which is also visible in the time series data of different cities and Kuwait, Figures 6 and 7). It suggests high variability in different climatic parameters that control the EWT magnitude in this region.

All eight cities and Kuwait exhibit declining EWT trends which are punctuated by seasonal oscillations (Figure 8). The calculated seasonal model has peak-to-peak amplitudes of 3.1 ± 1.5cm for Makkah, 1.75± 1.10 cm for Madina, 1.42±1.12 cm for Riyadh, 4.05± 1.1 cm for Damam, 5.98 ± 1.21 cm for Kuwait, 6.59± 1.31 cm for Dubai, 2.10± 0.98 cm for Alain, 1.42± 0.92 cm for Masqat and 7.61±2.1 cm for Sanaa. It suggests that inland areas receive less amount of precipitation as compared to most of the coastal areas (please see Figure 1 for locations of inland and coastal cities). The exception is Masqat, though it is a coastal city, it has the same signal amplitude as Riyadh. The rainfall data (Figure 9) also validates the modeled signal and the areas with higher modeled amplitude receive relatively higher amounts of rainfall. Furthermore, Figure 9 shows that there is a phase lag between the rainfall and EWT's positive peak at most locations where EWT follows the rainfall peak. The phase lag depends upon the timing of runoff. If the runoff is quick then the storage is mostly proportional to precipitation. If the runoff is very slow, the storage equals the integration of precipitation.

Regarding the long-period trends (Figures 6 and 7), the highest rate of decline is in Al Jouf, which corresponds to -1.69cm/year (R^2=0.95), and for Sanaa, it is the lowest -0.13cm/year (R^2=0.90). For Riyadh, it is -0.72cm/year (R^2=0.99), For Kuwait, the rate of decline is -0.19 cm/year (R^2=0.77) the data indicates this kind of declining trend is basically coming from a rapid EWT decline between 2005 and 2008. After this period the trend moves in a horizontal line. The rainfall data of Kuwait indicates no significant change in the seasonal component that can maintain the horizontal trend observed in the GRACE/GRACE-FO data. As compared to Makkah (the rate of EWT declined -0.36cm/year), Madina has a higher rate value of 0.48cm/year (R^2=0.99). Damam is also following the same linear decline trend at the rate of -0.48cm/year (R^2=0.94). In the UAE, Dubai and Alain also exhibit a declining EWT trend with a -0.19cm/year value with R^2 values of 0.90. It is interesting to note that for the various cities of Saudi Arabia, the decline rate can be explained by a linear regression model with an R^2 value of ≥ 0.94. However, outside of Saudi Arabia, though various cities indicate a strong fit between the model and trend, the R^2 value is relatively less for Kuwait and Alain, partly because their EWT trend has become horizontal in recent times. In contrast, in Sanaa Yemen in recent times (i.e. after 2020) the EWT seems declining as compared to the previous flat behavior. Othman and Abotalib, (2019) calculated the rate of EWT decline in the central Arabian Region which was 1 cm/

year, and Fallatah et al. (2018) conducted research on the aquifers of Al Jouf region and calculated the EWT decline trend using GRACE data and it was 1.1cm/year. However, our analysis indicates the decline in the Al Jouf area has now accelerated (Figure 7) and has a value of 1.69 cm/year with an R^2 value of 0.95 which is significantly faster than previous calculations (Fallatah et al. 2018; Othman and Abotalib, 2019). In Figure 6, panels a and c, one can clearly see two different trends, and in the recent data, it seems the decline is accelerating. When we decompose the trend into the two times and model them separately (Figure 6, panel d) then not only does the model fit improve i.e. from 0.95 to 0.98 (for 2002-2018 GRACE data) and to 0.99 (for 2019 to 2023 GRACE-FO data) but also we can find out that the rate of decline for Al Jouf region (in GRACE-FO data) is now 3.24 cm/year which is nearly the three times higher than the previous estimates (Fallatah et al. 2018; Othman and Abotalib, 2019).

3.2. Socioeconomic implications of the current water level decline, associated sustainability challenges, and established reversal methods

With the passage of time, the demand for fresh will continue to increase due to the following major reasons: (i) rapid increase in the population as discussed in section 1 (ii) boost of the tourism industry which is related to the steps towards "diversification of the economy" in which GCC countries want to create additional income industries and wants to reduce their reliance on the oil-based economy (Mishrif, 2017; Go¨ssling et al. 2012). Fresh water is needed to maintain the gardens, landscape, hotels, and theme parks (Hof and Schmitt 2011). However, the ever-increasing demand for water coupled with the effects of climate change is escalating pressure on water resources in the region (Odhiambo, 2016). The land use and agricultural maps at various locations of the Arabian Peninsula Region can be accessed from various studies including (Kamal et al. 2023; Qiaoqiao et al. 2024; Alshehri et al. 2024; Othman and Abotalib, 2019).

The Arabian Peninsula countries heavily depend upon imported food products and with the growth in population and tourism, the GCC countries are supporting their local farming in order to increase the food self-sufficiency percentage and reduce import-related food expenses. There are water-conserving ways to do farming (hydroponic systems and growing genetically modified crops that can grow in water scarcity) (Fiaz et. al. 2018). However, technology is not developed enough to scale up these ways to industrial scale. So there will be a continued mining of underground water reserves to meet the escalating demands.

The water level is declining and it is not only limiting the availability of this precious water resource but there are associated hazards like subsidence (Bockstiegel et al. 2023, Yao et al. 2023; Lei et al. 2023; Ghasemi, et al. 2023; Younas et al. 2023) which further complicates the efforts to achieve sustainability. As shown in the current research, there is a significant decline in the water reserves of the Arabian Peninsula and now we observed a sharp decline in the Al Jouf region in the latest data. It is important to note that the withdrawal rate of 1.1 cm/year has resulted in land subsidence (Othman, and Abotalib, 2019) and now the withdrawal rate is close to 1.8 cm/year in the cumulative data and it is 3.24 cm/year in the recent GRACE-FO data which are 43% and three times higher, respectively. It means that the land subsidence issue will further complicate agricultural, urban, and socio-economic sustainability. Furthermore, different studies conducted in various parts of the world indicate that the extensive withdrawal of underground degrades its quality as arsenic can reside within pore water of clay strata within aquifers and is released due to overpumping (Taneja et al. 2023; Smith et al. 2018; Harvey et al. 2002).

In 16% of the world's aquifer systems, groundwater level declines are reversed (Jaseko et al. 2024). For instance, in the Bangkok basin (Thailand), groundwater levels declined in the late 20th century but then began to rise in the early 21st century. This reversal has been linked to regulatory actions such as well licenses and groundwater pumping fees (World Bank, 2008). Following the introduction of regulated aquifer recharge projects, groundwater deepening has reversed in the west of Tucson, Arizona (Scanlon et al. 2016). Another example is the Abbas-e Sharghi basin in Iran, where water diverted from the Kharkeh Dam and reversed losses in groundwater levels during the 20th century (Karimi and Alimoradi, 2017). Recharge operations are sometimes only feasible in areas with excess surface water (Winter et al., 1998) so it is important to coordinate surface water and groundwater management. However, these instances show that interventions can turn around decreasing groundwater trends (Jaseko et al. 2024).

In the Arabian Peninsula Region, with the increasing demand in various sectors, one can foresee that water will become an increasingly scarce commodity. It is strongly possible that it would become a limiting factor for further social, agricultural, and industrial development. That's why major reviews and shifts are necessary in the current policies related to the population and reliance on imported food. At the same time, appropriate and drastic measures in water conservation are necessary.

4. Conclusions

In this research, we have focused on the Arabian Peninsula Region and have utilized GRACE/GRACE-FO MASCON, Global Land Data Assimilation System (GLDAS) soil moisture, and the Integrated

Multi-satellite Retrievals for Global Precipitation Mission (IMERG) rainfall data. We have conducted a detailed spatiotemporal evaluation of the highest EWT decline signals within the Arabian Peninsula Region. Also, we have analyzed the EWT signals for the 8 different cities and Kuwait of the Arabian Peninsula. The highest EWT decline is found in the Al Jouf Region where what decline shows a 60% faster decline (in the cumulative trend model) and a three times faster decrease (in the decomposed trend model) in the recent GRACE-FO data. It is interesting to note that for the various cities of Saudi Arabia, the decline rate can be explained by a linear regression model with an R^2 value of ≥ 0.95. Considering the short period (seasonal component), the water variability amplitudes are higher in the coastal cities (the exception is Muscat) as compared to inland areas. Also, for all the locations, in the recent data, one can observe higher seasonal amplitudes suggesting a higher variability in different climatic factors that control EWT magnitude. With the increasing demand for water in various sectors, one can foresee that water will become an increasingly scarce commodity. It would likely start to impede future advancements in the social, agricultural, and industrial sectors. That's why the current policies regarding population growth and reliance on imported food require significant assessments and changes. However, there is also a need for suitable and stringent water conservation measures. It is also an established fact that groundwater decline can be reversed with effective regulatory policies like well licenses and groundwater pumping fees. Furthermore, creating recharge wells strategically and directing the seasonal and torrential rainwater to the recharge wells can assist in minimizing the runoff and help in enhancing groundwater recharge. This research not only emphasizes on the severity of the water decline issue in the Arabian Peninsula Region but also highlights different under-stress water areas thus this study opens corridors for future in-situ field observation locations.

Acknowledgments

We are thankful to the anonymous reviewers for their constructive that helped to improve the manuscript. GRACE/GRACE-FO data for this research was accessed from the link https://www2.csr.utexas.edu/grace/RL06_mascons.html and the rainfall (IMERG) data was accessed from the link https://giovanni.gsfc.nasa.gov/giovanni/. The GLDAS data was acquired from (https://disc.gsfc.nasa.gov/datasets?keywords=GLDAS. The authors are thankful to the University of Texas, USA, and the National Aeronautics and Space Administration (NASA) for keeping the datasets online and free of cost.

Funding Information

This research has been funded by Zayed University, Abu Dhabi, UAE (Grant ID: 23021).

References

Alshehri, F.; Mohamed, A. (2023) Analysis of Groundwater Storage Fluctuations Using GRACE and Remote Sensing Data in Wadi As-Sirhan, Northern Saudi Arabia. Water 2023, 15, 282. https://doi.org/10.3390/w15020282

Alshehri F, Al-Hamid, HTA, Mohamed, A (2024) Mapping coastal groundwater potential zones using remote sensing based AHP model in Al Qunfudhah region along Red Sea, Saudi Arabia, Heliyon, doi: https://doi.org/10.1016/j.heliyon.2024.e28186

Al-Zubari WK (1998) Toward the establishment of a total water cycle management and re-use program in the GCC countries. In: Mahdi KA (ed) Water in the Arabian Peninsula, problems and policies. Ithaca Press, Reading, UK, pp 255–273, https://doi.org/10.1016/S0011-9164(98)00196-

Arora, M., Dixit, M. & Pateriya, B. (2022) Assessment of Water Storage Changes Using Satellite Gravimetry and GLDAS Observations over a Part of Indus Basin, India. Water Conserv Sci Eng 7, 623–645. https://doi.org/10.1007/s41101-022-00169-6

Attada, R.; Dasari, H.P.; Ghostine, R.; Kondapalli, N.K.; Kunchala, R.K.; Luong, T.M.; Hoteit, I. (2022) Diagnostic evaluation of extreme winter rainfall events over the Arabian Peninsula using high-resolution weather research and forecasting simulations. Meteorol. Appl. https://doi.org/10.1002/met.2095

Bachellerie IJ (2012) Renewable energy in the GCC Countries: resources, potential, and prospects. Gulf Research Center. http://library.fes.de/pdf-files/bueros/amman/09008.pdf. Accessed 10th October 2023

Bernauer, T., and Böhmelt, T. (2020). International Conflict and Cooperation over Freshwater Resources. Nat. Sustain. 3, 350–356. doi:10.1038/s41893-020-0479-8

Bockstiegel, M., Richard-Cerda, J.C., Muñoz-Vega, E. *et al.* Simulation of present and future land subsidence in the Rafsanjan plain, Iran, due to groundwater overexploitation using numerical modeling and InSAR data analysis. *Hydrogeol J* (2023). https://doi.org/10.1007/s10040-023-02657-y

Boretti, A., Rosa, L. (2019) Reassessing the projections of the world water development report. npj Clean Water 21 2, 1–6. https://doi.org/10.1038/s41545-019-0039-9

Chowdhury S, Champagne P (2006) Use of treated wastewater: evaluation of wastewater minimization strategies using fuzzy technique. In: Proceedings of the Conference on Advanced Technology in the Environmental Field (ATEF), Spain

Dai, Y., Zeng, X., Dickinson, R.E., Yang, Z.L., 2003. The common land model. Bull. Am.Meteorol. Soc. 84, 1013–1023. https://doi.org/10.1175/BAMS-84-8-1013

Daneshvar M, M.R., Ebrahimi, M. & Nejadsoleymani, H. (2019) An overview of climate change in Iran: facts and statistics. Environ Syst Res 8, 7. https://doi.org/10.1186/s40068-019-0135-3

Ditmar, P. Conversion of time-varying Stokes coefficients into mass anomalies at the Earth's surface considering the Earth's oblateness (2018). J Geod 92, 1401–1412. https://doi.org/10.1007/s00190-018-1128-0

Doll, ¨ P., 2009. Vulnerability to the impact of climate change on renewable groundwater resources: a global-scale assessment. Environ. Res. Lett. 4, 35006.

Economist Intelligence Unit (EIU) (2010) The GCC in 2020: resources for the future. a report from the economist intelligence unit sponsored by the qatar financial centre authority. http://graphics.eiu.com/upload/eb/GCC_in_2020_Resources_WEB.pdf. Accessed 10 October 2023.

Fallatah, O. A., Ahmed, M., Cardace, D., Boving, T., and Akanda, A. S. (2019). Assessment of Modern Recharge to Arid Region Aquifers Using an Integrated Geophysical, Geochemical, and Remote Sensing Approach. J. Hydrol. 569, 600–611. https://doi.org/10.1016/j.jhydrol.2018.09.061

Fallatah, O. A., Ahmed, M., Save, H., and Akanda, A. S. (2017). Quantifying Temporal Variations in Water Resources of a Vulnerable Middle Eastern Transboundary Aquifer System. Hydrol. Process. 2017, 1–11. https://doi.org/10.1002/hyp.11285

Fiaz S, Mehmood Ali Noor, Fahad Owis Aldosri (2018) Achieving food security in the Kingdom of Saudi Arabia through innovation: Potential role of agricultural extension, Journal of the Saudi Society of Agricultural Sciences, Volume 17, Issue 4, https://doi.org/10.1016/j.jssas.2016.09.001.

Gerten, D., Heck, V., Jägermeyr, J., Bodirsky, B. L., Fetzer, I., Jalava, M., et al. (2020). Feeding Ten Billion People Is Possible within Four Terrestrial Planetary Boundaries. Nat. Sustain. 3 (3), 200–208. https://doi.org/10.1038/s41893-019-0465-1

Ghasemi, A., Bahmani, O., Akhavan, S. et al. (2023) Investigation of land-subsidence phenomenon and aquifer vulnerability using machine models and GIS technique. Nat Hazards 118, 1645–1671. https://doi.org/10.1007/s11069-023-06058-y

Gössling S, Paul Peeters, C. Michael Hall, Jean-Paul Ceron, Ghislain Dubois, La Vergne Lehmann, Daniel Scott (2012) Tourism and water use: Supply, demand, and security. An international review,Tourism Management, https://doi.org/10.1016/j.tourman.2011.03.015.

Gronwall, ¨ J., Danert, K. (2020) Regarding Groundwater and Drinkingwater Access through a Human Rights Lens: Self-Supply as a Norm. Water (Switzerland), vol. 12. https://doi.org/10.3390/w12020419.

Harvey, CF, C.H. Swartz, A.B.M. Badruzzaman, N. Keon-Blute, W. Yu, M.A. Ali, J. Jay, R. Beckie, V. Niedan, D. Brabander, P.M. Oates, K.N. Ashfaque, S. Islam, H.F. Hemond, M.F. Ahmed Arsenic mobility and groundwater extraction in Bangladesh Science, 298 (2002), pp. 1602-1606, https://doi.org/10.1126/science.1076978

Hata, S., Sugiyama, S. & Heki, K. (2022) Abrupt drainage of Lago Greve, a large proglacial lake in Chilean Patagonia, observed by satellite in 2020. Commun Earth Environ 3, 190. https://doi.org/10.1038/s43247-022-00531-5

Hatamkhani A, Ahmad KhazaiePoul, Ali Moridi (2022) Sustainable water resource planning at the basin scale with simultaneous goals of agricultural development and wetland conservation. AQUA - Water Infrastructure, Ecosystems and Society 1 June 2022; 71 (6): 768–781. doi: https://doi.org/10.2166/aqua.2022.025

Hodrick, Robert; Prescott, Edward C. (1997). "Postwar U.S. Business Cycles: An Empirical Investigation" (PDF). Journal of Money, Credit, and Banking. 29 (1): 1–16. doi:10.2307/2953682. JSTOR 2953682.

Hof A, Thomas Schmitt (2011) Urban and tourist land use patterns and water consumption: Evidence from Mallorca, Balearic Islands, Land Use Policy,Volume 28, Issue 4, https://doi.org/10.1016/j.landusepol.2011.01.007.

Jasechko, S., Seybold, H., Perrone, D. et al., (2024) Rapid groundwater decline and some cases of recovery in aquifers globally. Nature 625, 715–721. https://doi.org/10.1038/s41586-023-06879-8

Jensen CB, Michael Gamborg, Kyle Raymond, John McGrath, Thorkild I.A. Sørensen, Berit L. Heitmann (2015) Secular trends in seasonal variation in birth weight, Early Human Development, Volume 91, Issue 6,https://doi.org/10.1016/j.earlhumdev.2015.03.010.

Kamal, H.J., Thomas, M., Abdulhadi, A. (2023). Perspectives of Geography, Environment, and Physiography of Kuwait. In: Suleiman, M.K., Shahid, S.A. (eds) Terrestrial Environment and Ecosystems of Kuwait . Springer, Cham. https://doi.org/10.1007/978-3-031-46262-7_2

Karimi, H. & Alimoradi, S. (2017) Impacts of water transfer from Karkheh Dam on rising of groundwater in Dasht-e-Abass Plain, Ilam Province. Res. Earth Sci. 8, 33–44.

Khaled Alghafli, Xiaogang Shi, William Sloan, Mohammad Shamsudduha, Qiuhong Tang, Ahmed Sefelnasr, Abdel Azim Ebraheem, (2023) Groundwater recharge estimation using in-situ and GRACE observations in the eastern region of the United Arab Emirates, Science of The Total Environment, Volume 867 doi: https://doi.org/10.1016/j.scitotenv.2023.161489.

Kong, F., Xu, W., Mao, R., Liang, D. (2022). Dynamic Changes in Groundwater Level under Climate Changes in the Gnangara Region, vol. 14. Water, Switzerland. https://doi.org/10.3390/w14020162. Western Australia.

Koster, R.D., Suarez, M.J., 1996. Energy and water balance calculations in the MosaicLSM. National Aeronautics and Space Administration, Goddard Space Flight. Center, Laboratory for Atmospheres, Data Assimilation Office: Laboratory for Hydrospheric Processes.

Koren, V., Schaake, J., Mitchell, K., Duan, Q.-Y., Chen, F., Baker, J.M., 1999. A parameterization of snowpack and frozen ground intended for NCEP weather and climate models. J. Geophys. Res. 104, 19569–19585. https://doi.org/10.1029/1999JD900232.

Landerer, F. W., Flechtner, F. M., Save, H., Webb, F. H., Bandikova, T., Bertiger, W. I., Bettadpur, S. V., Byun, S. H., Dahle, C., Dobslaw, H., Fahnestock, E., Harvey, N., Kang, Z., Kruizinga, G. L. H., Loomis, B. D., McCullough, C., Murböck, M., Nagel, P., Paik, M., Pie, N., Poole, S., Strekalov, D., Tamisiea, M. E., Wang, F., Watkins, M. M., Wen, H.-Y., Wiese, D. N., and Yuan, D.-N. (2020) Extending the Global Mass Change Data Record: GRACE Follow-On Instrument and Science Data Performance, Geophys. Res. Lett., 47, e2020GL088306, https://doi.org/10.1029/2020gl088306

Lei, K., Ma, F., Chen, B. *et al.* (2023) Effects of South-to-North Water Diversion Project on groundwater and land subsidence in Beijing, China. *Bull Eng Geol Environ* **82**, 18. https://doi.org/10.1007/s10064-022-03021-2

Liang, X., Lettenmaier, D.P., Wood, E.F., 1996. One-dimensional statistical dynamic representation of subgrid spatial variability of precipitation in the two-layer variable infiltration capacity model. J. Geophys. Res. 101, 21403. https://doi.org/10.1029/ 96JD01448.

Long D, Yanjun Shen, Alexander Sun, Yang Hong, Laurent Longuevergne, Yuting Yang, Bin Li, Lu Chen (2014) Drought and flood monitoring for a large karst plateau in Southwest China using extended GRACE data, Remote Sensing of Environment, https://doi.org/10.1016/j.rse.2014.08.006.

Long, D., Scanlon, B. R., Longuevergne, L., Sun, A. Y., Fernando, D. N., & Save, H. (2013). GRACE satellite monitoring of large depletion in water storage in response to the 2011 drought in Texas. Geophysical Research Letters, 40(13), 3395–3401. https://doi.org/10.1002/grl.50655

Luthcke, S.B., Sabaka, T.J., Loomis, B.D., Arendt, A.A., McCarthy, J.J., Camp, J., 2013.Antarctica, Greenland, and Gulf of Alaska land-ice evolution from an iterated GRACE global mascon solution. J. Glaciol. 59, 613–631. https://doi.org/10.3189/ 2013JoG12J147.

Mirkin B (2010) Population levels, trends and policies in the Arab region: challenges and opportunities. United Nations Development Programme Regional Bureau for Arab States, Arab Human Development Report. UNDP Research Paper Series, New York, USA

Mishrif, A. (2018). Introduction to Economic Diversification in the GCC Region. In: Mishrif, A., Al Balushi, Y. (eds) Economic Diversification in the Gulf Region, Volume I. The Political Economy of the Middle East. Palgrave Macmillan, Singapore. https://doi.org/10.1007/978-981-10-5783-0_1

Moghim, S. (2020) Assessment of Water Storage Changes Using GRACE and GLDAS. Water Resour Manage 34, 685–697. https://doi.org/10.1007/s11269-019-02468-5

Mohamed A, Abdelrahman K and Abdelrady A (2022) Application of Time-Variable Gravity to Groundwater Storage Fluctuations in Saudi Arabia. Front. Earth Sci. 10:873352. https://doi.org/10.3389/feart.2022.873352

Odhiambo, G.O. (2017) Water scarcity in the Arabian Peninsula and socio-economic implications. Appl Water Sci 7, 2479–2492. https://doi.org/10.1007/s13201-016-0440-1

Othman, A. (2019). "Measuring and Monitoring Land Subsidence and Earth Fissures in Al- Qassim Region, Saudi Arabia: Inferences from InSAR," in Advances in Remote Sensing and Geo Informatics Applications. CAJG 2018. Advances in Science, Technology & Innovation (IEREK Interdisciplinary Series for Sustainable Development). Editors H. El-Askary, S. Lee, E. Heggy, and B. Pradhan (Cham: Springer). doi:10.1007/978-3-030-01440-7_66

Othman, A., and Abotalib, A. Z. (2019). Land Subsidence Triggered by Groundwater Withdrawal under Hyper-Arid Conditions: Case Study from Central Saudi Arabia. Environ. Earth Sci. 78 (7), 243. doi:10.1007/s12665-019-8254-8

Qiaoqiao Jing, Jianjun He, Yarong Li, Xianyu Yang, Yue Peng, Hong Wang, Fei Yu, Jie Wu, Sunling Gong, Huizheng Che, Xiaoye Zhang (2024) Analysis of the spatiotemporal changes in global land cover from 2001 to 2020,Science of The Total Environment, Volume 908 doi: https://doi.org/10.1016/j.scitotenv.2023.168354

Ravn, MO, Harald Uhlig; On Adjusting the Hodrick-Prescott Filter for the Frequency of Observations. The Review of Economics and Statistics 2002; 84 (2): 371–376. doi: https://doi.org/10.1162/003465302317411604

Rodell, M., Famiglietti, J.S., Wiese, D.N. et al. (2018) Emerging trends in global freshwater availability. Nature 557, 651–659. https://doi.org/10.1038/s41586-018-0123-1

Rodell, M. and Famiglietti, J. S. (2001) An analysis of terrestrial water storage variations in Illinois with implications for the Gravity Recovery and Climate Experiment (GRACE), Water Resour. Res., 37, 1327–1339, https://doi.org/10.1029/2000WR900306

Rodell, M., Houser, P.R., Jambor, U., Toll, D., (2004). The global land data assimilation system. Bull. Am. Meteorol. Soc. 85, 381–394. https://doi.org/10.1175/BAMS-85-3-381.

Save, H., Bettadpur, S., Tapley B.D., (2016). High-resolution CSR GRACE RL05 mascons. Journal of Geophysical Research: Solid Earth. 121, 7547-7569. doi:10.1002/2016JB013007

Scanlon, B.R., Fakhreddine, S., Rateb, A. et al. (2023) Global water resources and the role of groundwater in a resilient water future. Nat Rev Earth Environ 4, 87–101. https://doi.org/10.1038/s43017-022-00378-6

Scanlon, B. R., Reedy, R. C., Faunt, C. C., Pool, D. & Uhlman, K. (2016) Enhancing drought resilience with conjunctive use and managed aquifer recharge in California and Arizona. Environ. Res. Lett. 11, 035013 DOI 10.1088/1748-9326/11/3/035013

Scanlon, B.R., Zhang, Z., Save, H., Wiese, D.N., Landerer, F.W., Long, D., Longuevergne,L., Chen, J., (2016) Global evaluation of new GRACE mascon products for hydrologic applications. Water Resour. Res. 52, 9412–9429. https://doi.org/10.1002/2016WR019494

Siebert, S., Burke, J., Faures, J. M., Frenken, K., Hoogeveen, J., Döll, P., et al. (2010). Groundwater Use for Irrigation - a Global Inventory. Hydrol. Earth Syst. Sci. 14, 1863–1880. https://doi.org/10.5194/hess-14-1863-2010

Smith, R., Knight, R. & Fendorf, S. Overpumping leads to California groundwater arsenic threat. *Nat Commun* **9**, 2089 (2018). https://doi.org/10.1038/s41467-018-04475-3

Tanaka Y and Heki, K. 2014Long- and short-term postseismic gravity changes of megathrust earthquakes from satellite gravimetry Geophys. Res. Lett., 41 (15) (2014), pp. 5451-5456 https://doi.org/10.1002/2014GL060559

Tanaka Y.S., Heki K., Matsuo K., Shestakov N.V., (2015). Crustal subsidence observed by GRACE after the 2013 Okhotsk deep-focus earthquake, Geophys. Res. Lett. 42(9), 3204–3209. 10.1002/2015GL063838

Taneja S, Yadav S, Pipil S, Karaca, HO, Haritash, A.K. (2023). Soil–Water Interactions and Arsenic Enrichment in Groundwater. In Hydrogeochemistry of Aquatic Ecosystems (eds S. Madhav, V.B. Singh, M. Kumar and S. Singh). https://doi.org/10.1002/9781119870562.ch5

Tapley, B.D., Bettadpur, S., Ries, J.C., Thompson, P.F., Watkins, M.M., 2004. GRACE measurements of mass variability in the Earth system. Science 305, 503–505. https://doi.org/10.1126/science.1099192.

Taylor, R.G., Villholth, K.G., Vor ¨ osmarty, ¨ C.J., Zheng, C., 2023. Global water resources and the role of groundwater in a resilient water future. Nat. Rev. Earth Environ. 4, 87–101. https://doi.org/10.1038/s43017-022-00378-6.

Trondalen (2009). "Climate Changes, Water Security and Possible Remedies for the Middle East. From Potential Conflict to Co-operation Potential," in The United Nations World Water Development Report 3, Water in a Changing World. The United Nations Educational, Scientific and Cultural Organization, 7: University of Texas at Austin

UNESCO-WWDR (2003). Water for People. Water for Life. The United Nations World Water Development Report (WWDR). http://unesdoc.unesco.org/images/0012/001297/129726e.pdf. Accessed on 10 October 2023

UN-ESCWA; BGR (2013). United Nations economic and social commission for western Asia; Bundesanstaltfu¨ r Geowissenschaften und Rohstoffe. Beirut, Lebanon: Inventory of Shared Water Resources in Western Asia.

Velicogna I, Wahr J (2005) Greenland mass balance from GRACE. Geophys Res Lett, 2005, 32: 18505. https://doi.org/10.1029/2005GL023955

Velicogna, I. (2009). Increasing rates of ice mass loss from the Greenland and Antarctic ice sheets revealed by GRACE. Geophysical Research Letters, 36, L19503. https://doi.org/10.1029/2009GL040222

Velicogna, I., Mohajerani, Y., Landerer, F., Mouginot, J., Noel, B., Rignot, E., et al. (2020). Continuity of ice sheet mass loss in Greenland and Antarctica from the GRACE and GRACE follow-on missions. Geophysical Research Letters, 47(8), e2020GL087291. https://doi.org/10.1029/2020GL087291

Wada, Y., Van Beek, L. P. H., Van Kempen, C. M., Reckman, J. W. T. M., Vasak, S., and Bierkens, M. F. P. (2010). Global Depletion of Groundwater Resources. Geophys. Res. Lett. 37 (20). doi:10.1029/2010gl044571

Water UN (2012) Global Annual Assessment of Sanitation and drinking-water (GlAAS) 2012 report: the challenge of extending and sustaining services. UN, New York

Wahr, J., Molenaar, M., Bryan, F., 1998. Time variability of the Earth's gravity field Hydrological and oceanic effects and their possible detection using GRACE. J. Geophys. Res. 103, 30205–30229. https://doi.org/10.1029/98JB02844.

Watkins, M.M., Wiese, D.N., Yuan, D., Boening, C., Landerer, F.W., 2015. Improved methods for observing Earth's time-variable mass distribution with GRACE using spherical cap mascons. J. Geophys. Res. Solid Earth 120, 2648–2671. https://doi.org/10.1002/2014JB011547

Wiese, D.N., Landerer, F.W., Watkins, M.M., 2016. Quantifying and reducing leakage errors in the JPL RL05M GRACE mascon solution. Water Resour. Res. 52, 7490–7502.https://doi.org/10.1002/2016WR019344.

Winter, T. C., Harvey, J. W., Franke, O. L. & Alley, W. M. (1998) Ground water and surface water: a single resource. U.S. Geological Survey Circular 1139. https://doi.org/10.3133/cir1139 (1998).

World Bank, (2008) Buapeng, S. & Foster, S. Controlling groundwater abstraction and related environmental degradation in metropolitan Bangkok – Thailand. World Bank Case Profile Collection No. 20. https://documents1.worldbank.org/curated/en/750761468304831965/pdf/518250BRI0Box31GWMATE1CP1201Bangkok.pdf

World Bank (2005) A Water Sector Assessment Report on the Countries of the Cooperation Council of the Arab States of the Gulf. World Bank Report No. 32539-MNA, Washington, DC.

World Population Review (2024) Arabian Peninsula Countries 2024. https://worldpopulationreview.com/country-rankings/arabian-peninsula-countries

Wouters, B., Chambers, D., & Schrama, E. J. O. (2008). GRACE observes small-scale mass loss in Greenland. Geophysical Research Letters, 35(20), L20501. https://doi.org/10.1029/2008GL034816

Xavier L, M. Becker, A. Cazenave, L. Longuevergne, W. Llovel, O.C. Rotunno Filho, (2010) Interannual variability in water storage over 2003–2008 in the Amazon Basin from GRACE space gravimetry, in situ river level and precipitation data, Remote Sensing of Environment, https://doi.org/10.1016/j.rse.2010.02.005.

Yao, Y.; Li, S.; Jia, X.; Song, J.; Yue, D.; Zhang, Q.; Xiang, H (2023) Numerical Simulation of Ground Subsidence Response Conditional on Geothermal Exploitation in a Karst Reservoir Area of North China. *Sustainability*, *15*, 8089. https://doi.org/10.3390/su15108089

Younas M, Shuhab D. Khan, Osman Tirmizi, Younes Hamed (2023) Geospatial analytics of driving mechanism of land subsidence in Gulf Coast of Texas, United States, Science of The Total Environment, Volume 902, https://doi.org/10.1016/j.scitotenv.2023.166102

Ziyun Wang, Bao Zhang, Yibin Yao, (2023) Wei Zhang, GRACE and mass budget method reveal decelerated ice loss in east Greenland in the past decade, Remote Sensing of Environment, Volume 286, https://doi.org/10.1016/j.rse.2023.113450.

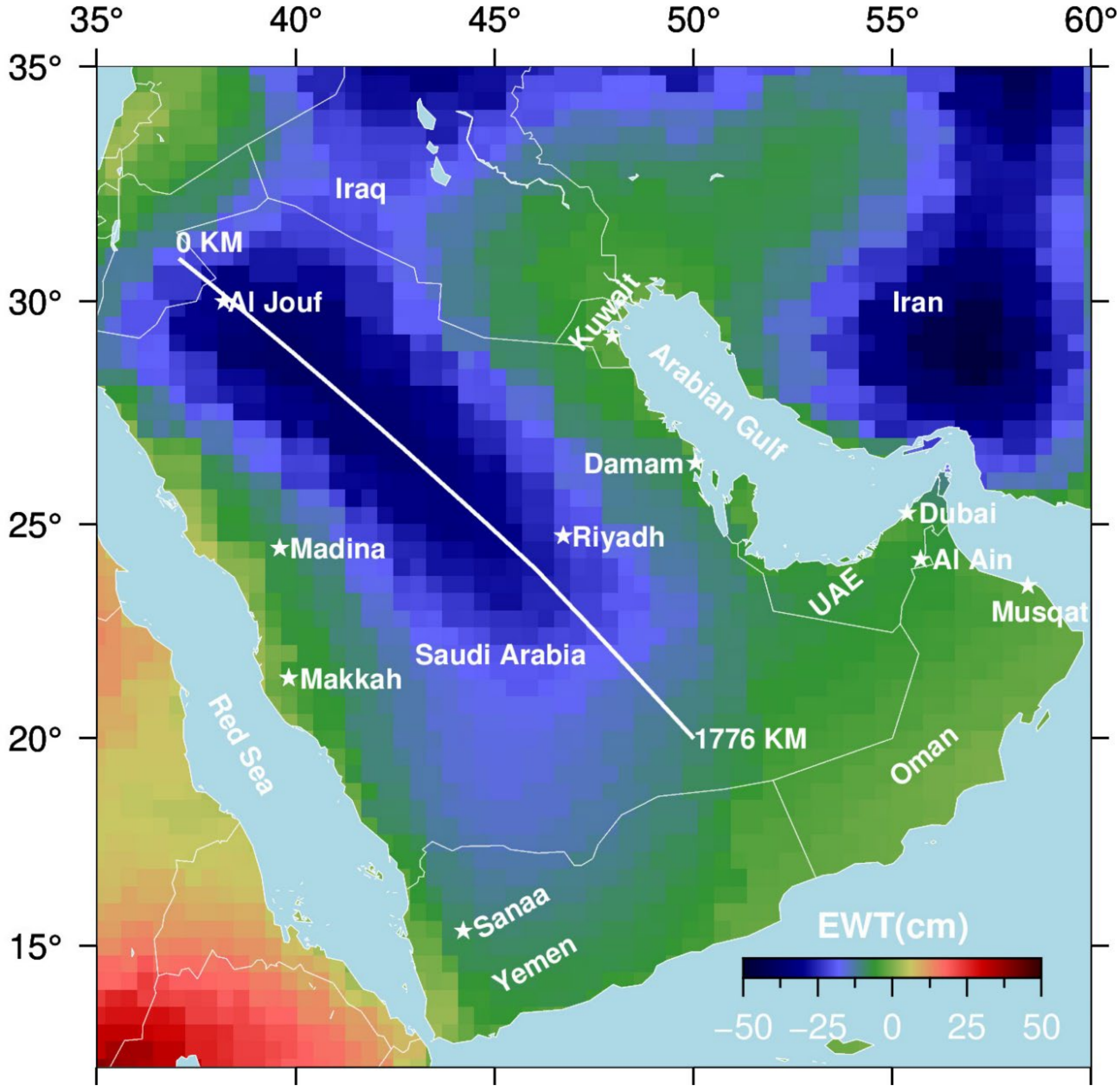

Figure 1. Study area. The background map indicates the secular Equivalent Water Thickness (EWT) created by subtracting the January 2003 data from the January 2023 data. The EWT values were extracted along the white line (Al Jouf-Riyadh Transect) (Figures 3, 4, and 5). In this Figure, the surface water bodies (oceans and lakes) have been masked and are indicated with a light blue color.

The star indicates the location of different cities, Kuwait and Aljouf Area from where time-series was extracted and analyzed (Figures 6, 7, and 8). The latitudes and longitudes of the extracted time series at all the locations (with white star) are: Makkah= 21.41N, 39.85E; Madinah= 24.49N, 39.62E; Riyadh= 24.71N, 46.75E; Damam= 26.40N, 50.03E; Al Joug(30.07N, 39.42E). Kuwait= 29.39N, 47.52E; Dubai= 25.07N, 55.34E; Al Ain= 24.17N, 55.67E; Musqat= 23.58N, 58.41E, Sanaa= 15.37N, 44.21E.

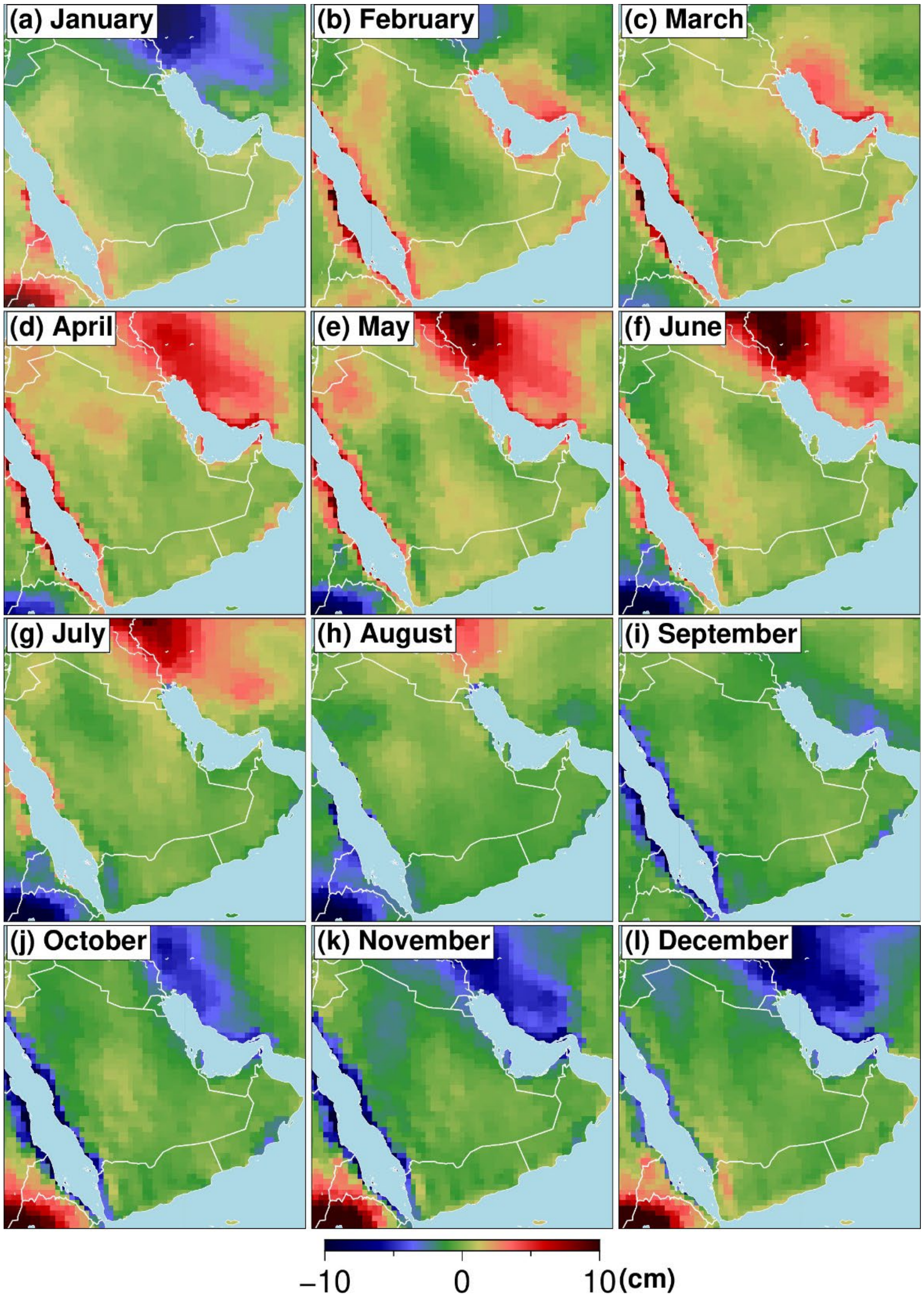

Figure 2. The seasonal maps for all the months of the year. This map displays the seasonal EWT change during a typical year. The seasonality component has been extracted using the HP- filter and its mean has been calculated and plotted here for all the available datasets. In this Figure, the surface water bodies (oceans and lakes) have been masked and are indicated with a light blue color.

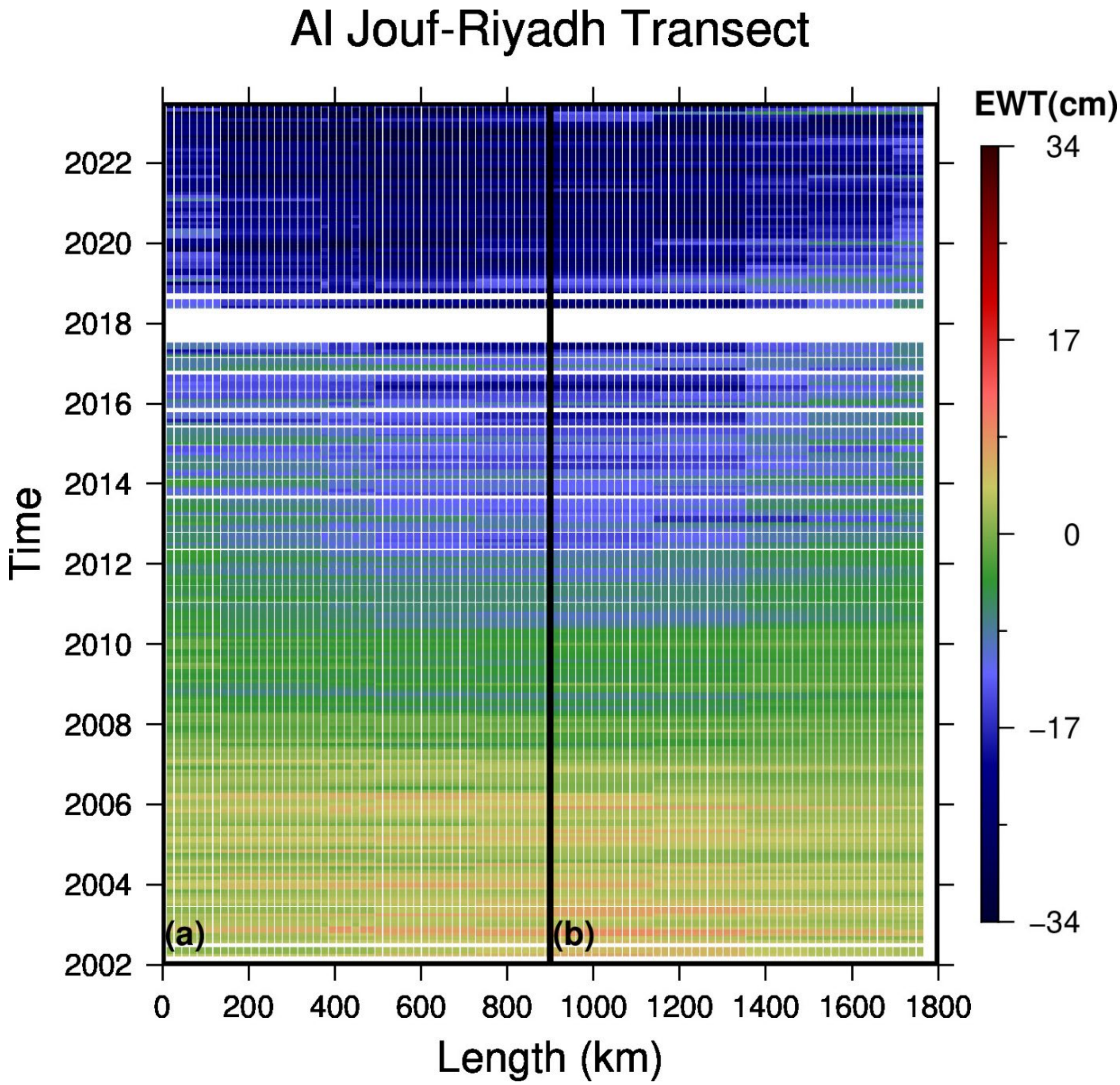

Figure 3. Spatio-temporal map of the extracted along Aljouf-Riyadh Transect (Fgure 1) (the area of strongest gravity decline within the Arabian Peninsula Region). These values are extracted along the white line indicated in Figure 1. This is the original data and contains both short-period (cyclic) and long-period components. The figure has been divided into two panels (a) 0-900 km and (b) 900-1800 km to observe the movement of the EWT signal.

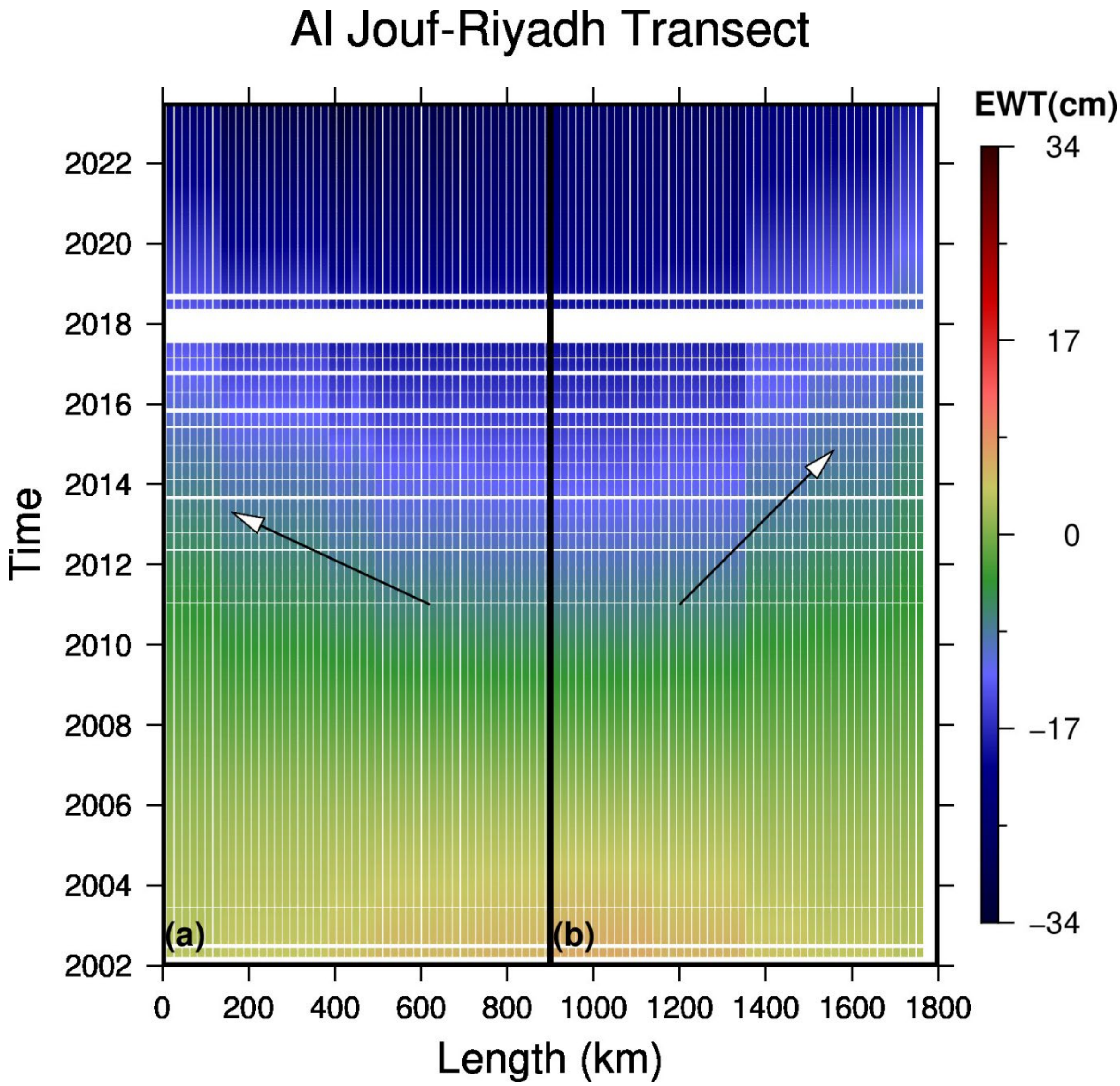

Figure 4. Spatio-temporal trend map of the Ajouf- Riyadh Transect (Figure 1), the area of strongest gravity decline within the Arabian Peninsula Region. The long-term component was extracted using the HP filter. The figure has been divided into two panels (a) 0-900 km and (b) 900-1800 km to observe the porpagation speed of EWT signal. The angle of the slant of the arrows indicate the speed of propagation.

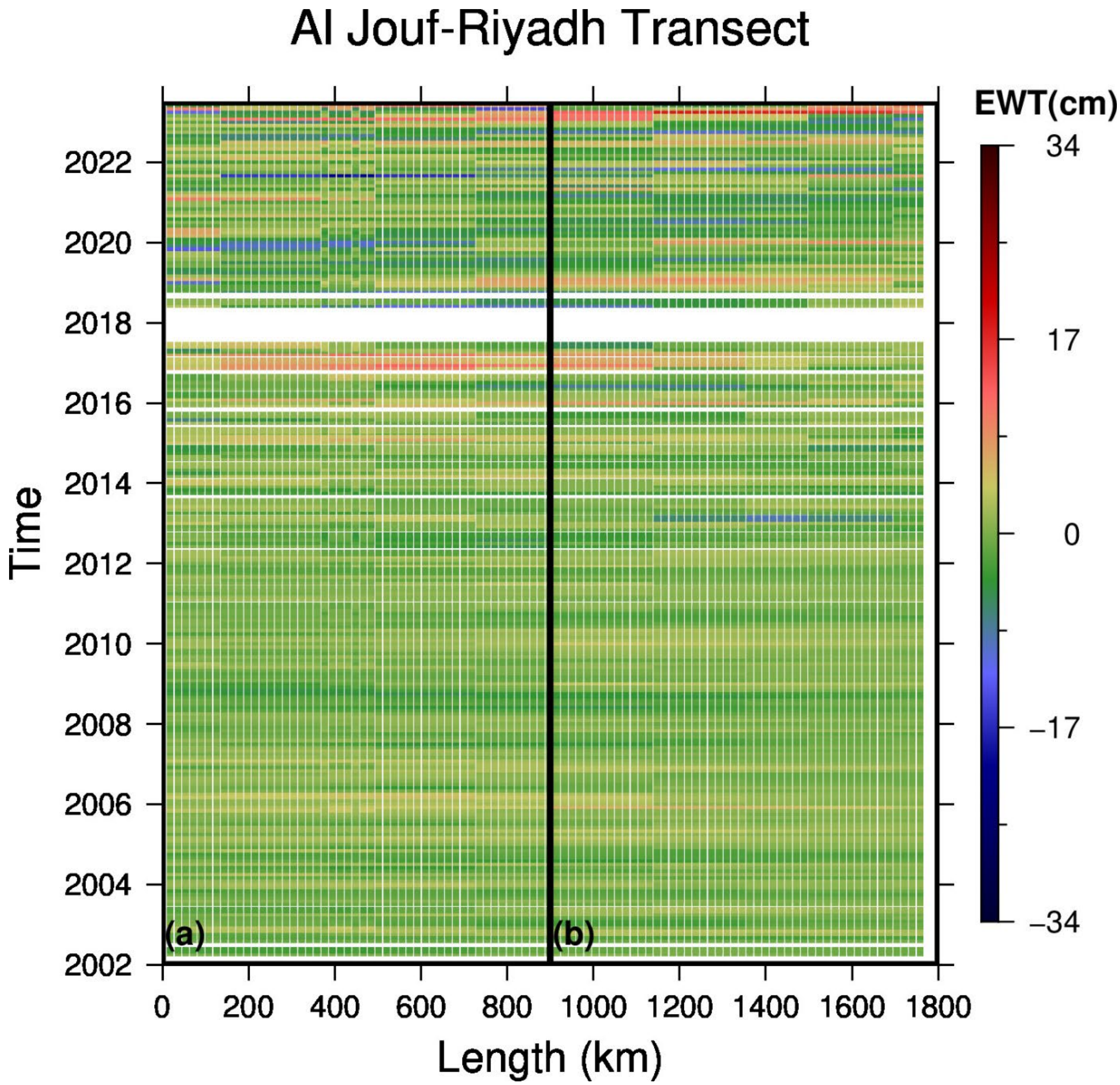

Figure 5. Spatio-temporal short-period intera-annual variability map of the Ajouf- Riyadh Transect (Figure 1), the area of strongest gravity decline within the Arabian Peninsula Region. The long-period component is removed from the raw data using HP filter.

.

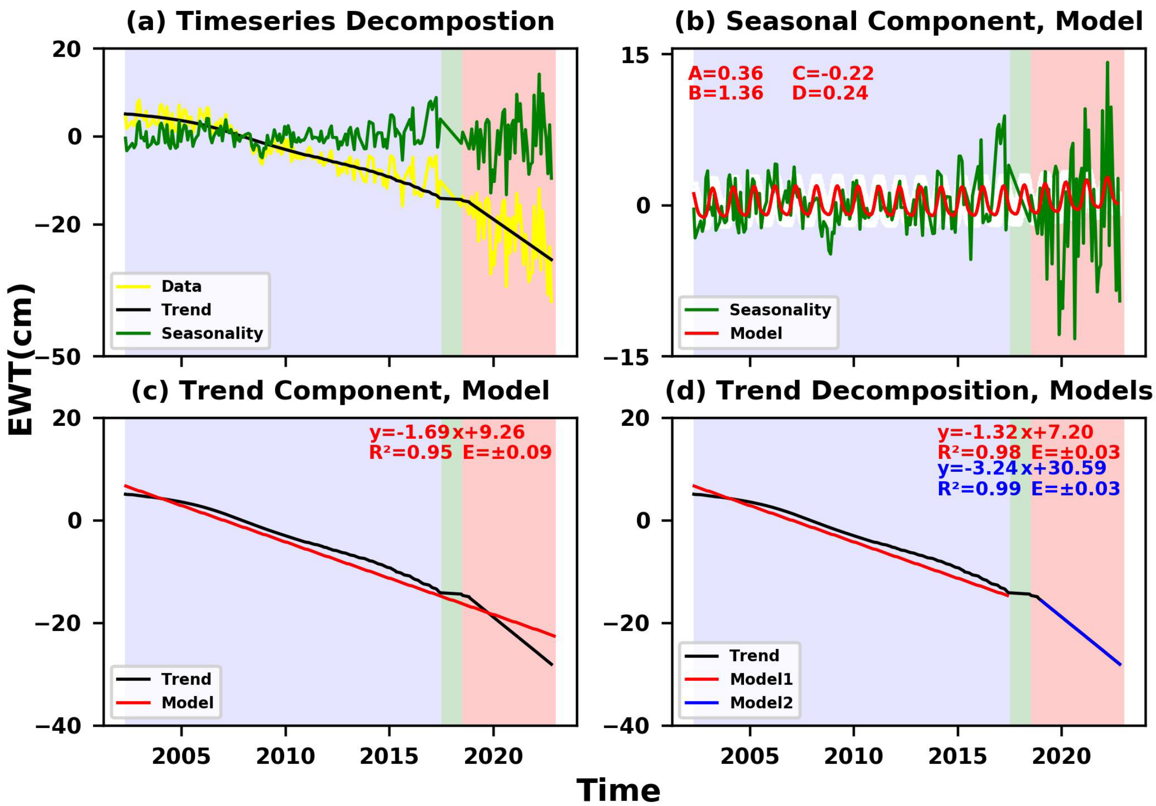

Figure 6. Groundwater EWT MASACON GRACE/GRACE-FO data (soil moisture component is subtracted) of the Al Jouf Area. The trend and seasonal components were extracted using the HP filter. The background colors indicate the different times of data acquisition i) light blue=GRACE time series data ii) light green=no data time iii) pink color=GRACE-FO time-series data. Figure panels show these details (a) data decomposition (b) seasonal component with its least square fit model (c)Long-period component with its linear regression model, coefficient of determination (R^2), and error value (E) (d) Decomposition of long-period component into two times for i.e. for GRACE (red model line) and GRACE-FO (blue model line).

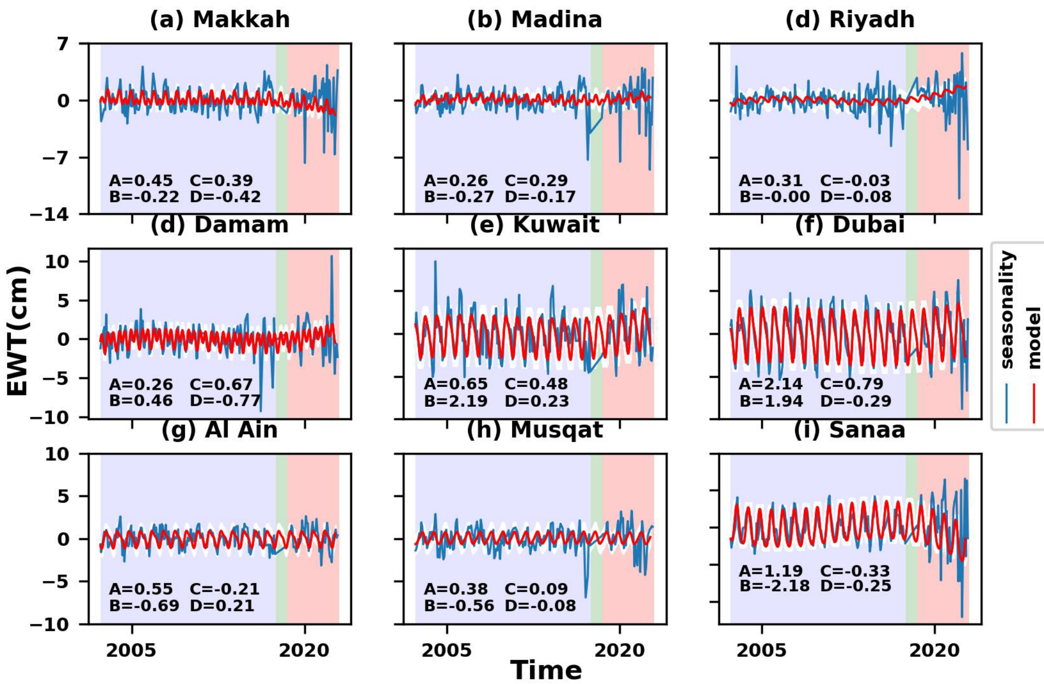

Figure 7. The cyclic (intra-annual) component (extracted using HP filter) of the MASCON data (soil moisture component is subtracted) for different places of the Arabian Peninsula Region (please see figure 1 for these locations). The numbers indicate the values of annual and biannual cosines (A and C) and sines (B and D). The background colors indicate the different times of data acquisition i) light blue=GRACE time series data ii) light green=no data time iii) pink color=GRACE-FO time-series data. In the figures, white curves indicate the confidence interval for the models which is based on errors.

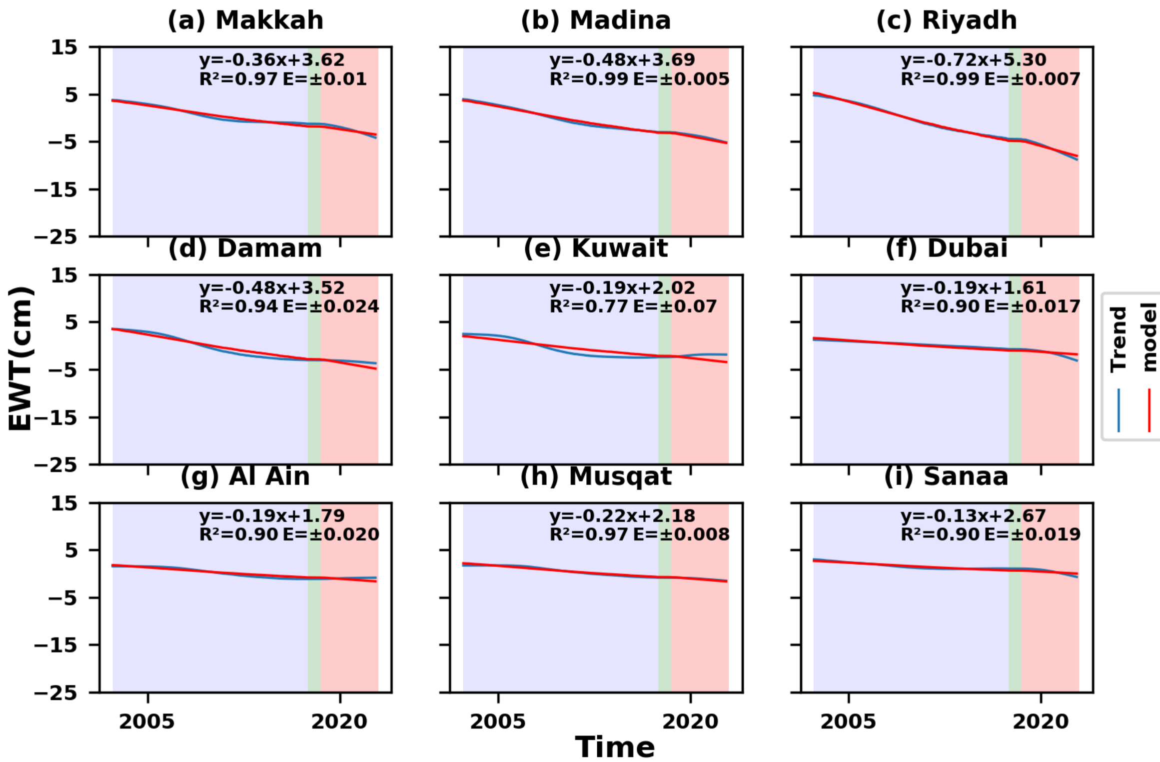

Figure 8. The long-period component (extracted using HP filter) of the MASCON data (soil moisture component is subtracted) for different places of the Arabian Peninsula Region (please see Figure 1 for these locations). The linear regression model along with R^2 and error value (E) values are given for each location. The background colors indicate the different times of data acquisition i) light blue=GRACE time series data ii) light green=no data time iii) pink color=GRACE-FO time-series data.

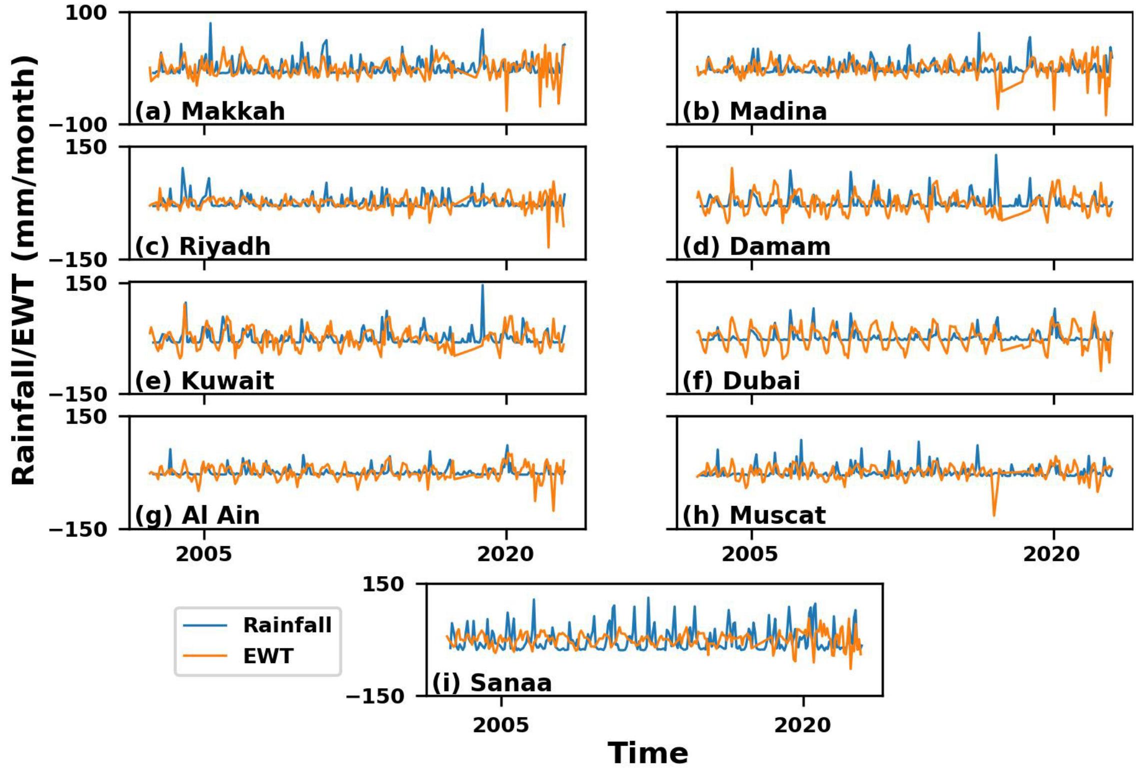

Figure 9. The rainfall data of the GPM and EWT data (intra-annual short-period component) of GRACE/GRACE-FO satellites for diffetent locations of the Arabian Peninsula Region.